Coastal Erosion from Space

Algorithm Theoretical Baseline Document

Ref: SO-TR-ARG-003-055-009-ATBD-ER

Date: 06/12/2019

Customer: ESA

Contract Ref.: 4000126603/19/I-LG

This page is intentionally left blank

Version and Signatures

Version	Date	Modification
0.1	27/11/2019	Template creation
0.2	29/11/2019	Gilbert notes
0.2	02/12/2019	Review and comments Colour: acronyms
0.3	04/12/2019	Review
0.4	05/12/2019	Gilbert complements
0.4	06/12/2019	Review
Verification by		
Authorisation		

Acronyms

BTM: Bathy Topo Model

CNES: Centre National d'Etudes Spatiales (French national Space Centre)

DEM: Digital Elevation Models

Dir: mean Direction of incident waves

DoC : Depth of Closure

DSAS : Digital Shoreline Analysis System

EBP : Equilibrium Beach Profile

EO : Earth Observation

EPR: End Point Rate (of a Shoreline)

EW : Extra Wide swath (SAR)

GPS-PPK: Global Positioning System (post-processing kinematic mode)

GRD: Ground Range Detected (level 1product – Sentinel 2)

Hs : Significant Height (wave parameter)

IW : (Interferometric Wide swath (SAR)

LRR : Linear Regression Rate

MSI: Multi Spectral Instrument (Sentinel 2)

NSM: Net Shoreline Movement (of a Shoreline)

OSW: Ocean Swell spectra (level 2 product – Sentinel 2)

SAR (Synthetic Aperture Radar)

SCE: Shoreline Change Envelope

SDS : satellite Derived Shoreline

SLC: Single Look Complex (level 1product – Sentinel 2)

SWAN: Simulating WAves Nearshore (numerical model of wave propagation)

TOA: Top Of Atmosphere

Tp : peak period (on a wave spectrum)

WLR: Weighted Linear Regression

WV: Wave mode (SAR)

Applicable and reference documents

Id	Description	Reference
AD-1	Requirement Baseline Document	SO-RP-ARG-003-055-006-RBD_v1.0_20190916
AD-2	Pre-processing ATBD	SO-TR-ARG-003-055-009-ATBD-PP

Contents

Version and Signatures ---------- **1**

Acronyms ---------- **2**

Applicable and reference documents ---------- **4**

List of Figures ---------- **6**

List of Tables ---------- **6**

1 Overview and Background Information ---------- **9**

1.1 Product requirement ---------- 9

1.2 Feasibility study ---------- 9

1.3 Potential Solutions ---------- 16

1.4 Product Specifications ---------- 18

2 Algorithm Description ---------- **19**

2.1 Data Processing outline ---------- 19

2.2 Algorithm Input ---------- 20

2.3 Theoretical Description of the models in background of the procedure ---------- 21

2.4 Algorithm output ---------- 23

2.5 Algorithm Performance Estimates ---------- 28

2.6 Products Validation ---------- 30

3 Conclusion ---------- **32**

3.1 Assessment of limitations ---------- 32

3.2 Mitigation ---------- 33

4 References ---------- **34**

5 Appendix ---------- **35**

List of Figures

Figure Description Page

Figure 1.1: The measurement distance from the baseline to each intersect point; this distance is used in conjunction with the corresponding shoreline date to compute the change-rate statistics. 11

Figure 1.2 : An example of how to place a baseline onshore, offshore, or through the data (mid-shore). The resulting transects will intersect the shorelines, regardless of placement. Baselines in a dataset may be all of one type or a combination of all three. 12

Figure 1.3 : A shoreline dataset (baseline [black], transect [gray], and shorelines and intersects [multicolor]) to describe the relationship between time and space data on the map, and as presented in a graphical form as distance from the baseline versus the shoreline date. The linear regression rate (LRR) was determined by plotting the shoreline intersect positions (distance from baseline) with respect to time (years) and calculating the linear regression equation of y = 1.34x − 2587.4. The slope of the equation describing the line is the rate (1.34 meters per year). 13

Figure 2.1: Sketch of the computer program for erosion rate calculation 19

Figure 2.2: Experimental variogram (black dots) and theoretical variogram (curve). 22

Figure 2.3: Empirical semi-variogram (converted to units of meters) for a transec at Narrabeen-Collaroy (NA1). It shows typical cross-shore shoreline variability at different timescales, from monthly lags to 10 years lags. The dashed grey line is a smooth fit across the data points. The range and sill are also indicated on the figure (in Vos et al, 2019). 24

Figure 2.4 : Representation of EBP through Eq. (5). The profile is the lower boundary for the volume of water per unit width above the sand. Given h^* as a function of y^*, the volume per unit width of water can be calculated by definite integral of y^* over the interval of [0, 1] (in Riazi & Türker, 2017). 24

Figure 2.5: Representation of erosion rates on point entities. 27

Figure 2.6 : Overall erosion rates estimated for each kilometre of the Andalusian coast (in Prieto-Campos, 2018). 27

Figure 2.7: Signal-to-noise ratio analysis across different timescales. Values of SNR above the threshold of 1 denote shoreline signals that are increasingly dominant over the measurement error (in Vos et al, 2019) 29

List of Tables

Table **Description** **Page**

No table of figures entries found.

1 Overview and Background Information

1.1 Product requirement

1.1.1 Information content quality and value

End users are interested in Coastal change indicators and in a description of coastal change at different scale. A description of change in sediment volume across the shore may be represent using an erosion rate that show accretion or erosion for a specified time range.

Product will allow management authorities of flood and coastal erosion risk to create a coastal erosion baseline from which decisions can be made. For planning and management purposes in coastal areas, specific managers could customize their own views based on their own interest and practices.

1.1.2 Product order & delivery services

Products will be available on a geoportal and delivery will be available by an ftp transfer.

The product will have to be compatible with help tools to facilitate the interpretation and analysis of the erosion rates: commercial software and open source GIS: ArcGIS MapInfo, QGIS, ect.

1.2 Feasibility study

1.2.1 Satellite sensors and mission

Please refer to the pre-processing ATDB (ref: SO-TR-ARG-003-055-009-ATBD-PP)

1.2.2 Existing EO Products

Please refer to the pre-processing ATDB (ref: SO-TR-ARG-003-055-009-ATBD-PP)

1.2.3 Models specification

Numerous observations of shoreline variability are essential to quantify long-term coastal erosion/accretion trends due to a range of factors: wind, waves, nearshore currents, etc. Most of the time, in *Coastal Engineering*, the shoreline is idealised as the “dynamic” interface between water and land. Nowadays robust and generic algorithm exist to automatically extract the shoreline on space-

borne observations and EO satellites provide a such potentially rich source of long-term historical shoreline datasets. EO observations were used to characterized shoreline changes at different spatial and temporal scale, Almonacid-Caballer et al. (2016)[1] characterised mid-term changes in annual mean while Liu et al. (2017)[2] monitor changes in annual mean width of a wave dominated beach. Hagenaars et al. (2018)[3] analysed the spatial variability in erosive/accretive yearly trends after a large-scale nourishment. (Xu, 2018)[4] quantified the yearly rate of shoreline change in the Gulf of Mexico using the Landsat archive.

The Digital Shoreline Analysis System (DSAS)[5] use a variety of shoreline to compute change statistics, from a drawn baseline, distance measurements for each intersect point on the shorelines are calculate in conjunction with the corresponding shoreline date.

[1] Jaime Almonacid-Caballer, Elena Sánchez-García, Josep E. Pardo-Pascual, Angel A. Balaguer-Beser, Jesús Palomar-Vázquez (2016): Evaluation of annual mean shoreline position deduced from Landsat imagery as a mid-term coastal evolution indicator. *Marine Geology Marine Geology* **372**, 79–88

[2] Qingxiang Liu, John Trinder, and Ian L. Turner (2017): Automatic super-resolution shoreline change monitoring using Landsat archival data: a case study at Narrabeen–Collaroy Beach, Australia. *Journal of Applied Remote Sensing*. Jan–Mar 2017. Vol. 11(1).

[3] Hagenaars, G., de Vries, S., Luijendijk, A.P., de Boer, W.P., Reniers, A.J.H.M. (2018): On the accuracy of automated shoreline detection derived from satellite imagery: A case study of the sand motor mega-scale nourishment. *Coast. Eng*. **133**, 113–125.

[4] Nan Xu (2018): Detecting Coastline Change with All Available Landsat Data over 1986–2015: A Case Study for the State of Texas, USA. *Atmosphere*, **9**, 107

[5] https://www.usgs.gov/centers/whcmsc/science/digital-shoreline-analysis-system-dsas?qt-science_center_objects=0#qt-science_center_objects

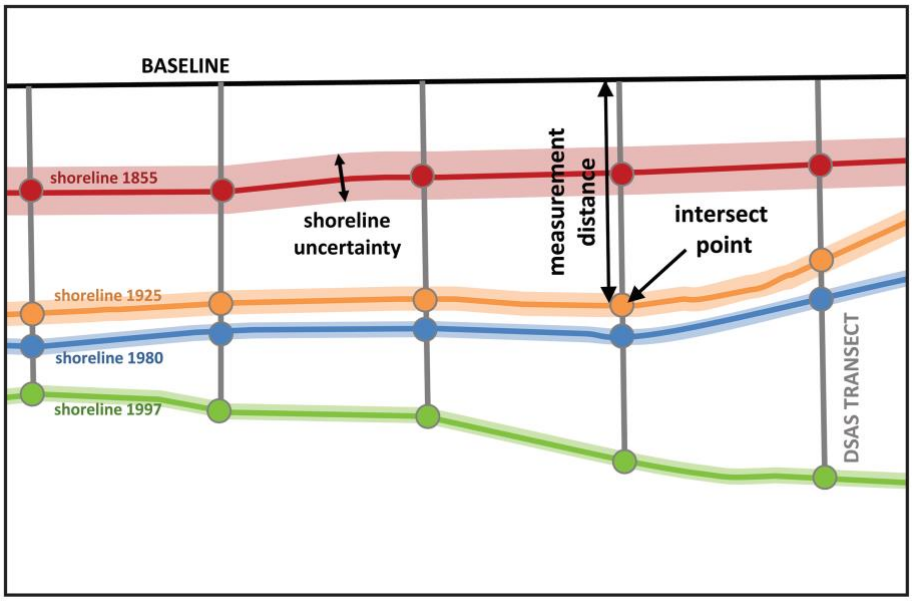

Figure 1.1: The measurement distance from the baseline to each intersect point; this distance is used in conjunction with the corresponding shoreline date to compute the change-rate statistics.

The baseline is constructed by the user and serves as the starting point for all transects cast by the DSAS application. Transects intersect each shoreline to create a measurement point, and these measurement points are used to calculate shoreline change rates. For shoreline change statistics to be computed, each shoreline must have a positional uncertainty associated with it.

Users have the option of specifying for each shoreline an overall uncertainty value, which should account for both positional and measurement uncertainties. The shoreline uncertainty is incorporated into the calculations for the standard error, correlation coefficient, and confidence intervals, which are provided for the simple and weighted linear regression methods (linear regression rate [LRR] and weighted linear regression [WLR] attributes in rate file, respectively).

In DSAS v5.0[6], the baseline can be drawn anywhere relative to the shoreline data, even between and among shoreline positions (**Error! Reference source not found.**). While there are a wide variety of shoreline proxies that can be used to represent the shoreline position at a specific point in time, DSAS

[6] USGS (2018) Digital Shoreline Analysis System (DSAS) Version 5.0 User Guide. US geological Survey – Open file 2018-1179

v5.0 only recognizes mean high water (MHW) and high-water line (HWL). When these two shoreline types are present DSAS performs a proxy-datum bias correction.

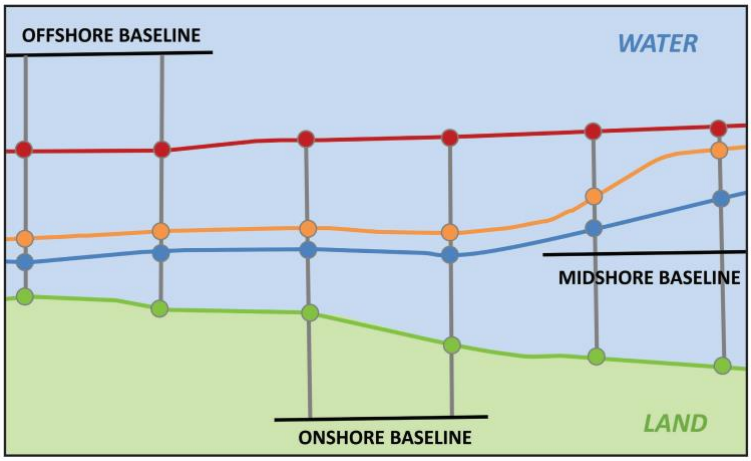

Figure 1.2 : An example of how to place a baseline onshore, offshore, or through the data (mid-shore). The resulting transects will intersect the shorelines, regardless of placement. Baselines in a dataset may be all of one type or a combination of all three.

Within this method, the different rates are expressed as meters of change per year as measured along the transects. The Shoreline Movement (NSM) is calculated according to the distance between the oldest and the youngest shorelines for each transect. The Shoreline Change Envelope (SCE) reports a distance. The SCE value represents the greatest distance among all the shorelines that intersect a given transect; the End Point Rate (EPR) is calculated by dividing the distance of shoreline movement by the time elapsed between the oldest and the most recent shoreline. And a linear regression rate-of-change (LLR) statistic can be determined by fitting a least-squares regression line to all shoreline points for a transect.

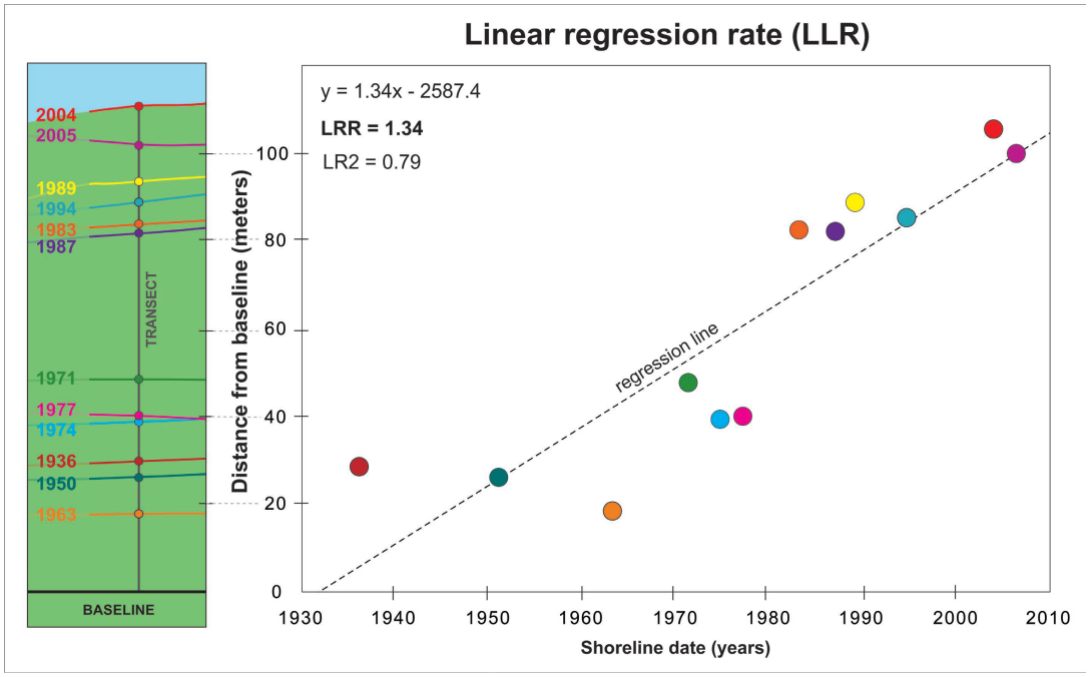

Figure 1.3 : A shoreline dataset (baseline [black], transect [gray], and shorelines and intersects [multicolor]) to describe the relationship between time and space data on the map, and as presented in a graphical form as distance from the baseline versus the shoreline date. The linear regression rate (LRR) was determined by plotting the shoreline intersect positions (distance from baseline) with respect to time (years) and calculating the linear regression equation of y = 1.34x – 2587.4. The slope of the equation describing the line is the rate (1.34 meters per year).

The predicted (or estimated) values of *y* (the distance from baseline) are computed for each shoreline point by using the values of *x* (the shoreline date) and solving the equation for the best-fit regression line:

$$y = mx + b$$

y is the predicted distance from baseline,

m is the rate of change,

b is *y*-intercept (where the line crosses the *y*-axis).

The standard error of the estimate measures the accuracy of the predicted values of *y* by comparing them to known values from the shoreline point data.

It is defined as LSE for ordinary linear regression and WSE for weighted linear regression:

$$LSE \text{ or } WSE = \sqrt{\frac{\Sigma(y-y')^2}{n-2}}$$

y is known distance from baseline for a shoreline data point, *y'* is predicted value based on the equation of the best-fit regression line, and *n* is number of shorelines used.

Other methods are using multitemporal and multiresolution data, linked with post-processing kinematic global positioning system (PPK GPS) surveys to study short and long-term effect of the shoreline change the processes controlling the persistent horizontal and vertical erosion[7]. The three main steps of this method are, first, the installation of local geodetic stations to support field surveys, a plani-altimetric survey of the beach face using geodetic GPS for shoreline definition, and the computation of Digital Elevation Models (DEM) to calculate sediment volume of erosion/accretion. From the DEMs, are establish several cross-shore profiles with an appropriate level of precision. Then, a sequential DEM of the same area can be generated for change detection purposes or to estimate volume balance and sediment accretion or erosion rates.

1.2.4 Auxiliary data

Two kind of data are usually used in a shoreline inference procedure:

1- MetOcean data

- Wave parameters: significant height (Hs), Peak period (Tp), direction of waves (Dir);
- Sea Surface Height (storm surge, tide, …);
- Wind (Speed & Direction, pressure).

Water level measurements include most of the time both tide, surge and waves information from measurement stations. Some studies are using water levels data at the satellite imagery acquisition

[7] VENERANDO EUSTA´ QUIO AMARO, LI´VIAN RAFAELY SANTANA GOMES, FRANCISCO GABRIEL FERREIRA DE LIMA, ADA CRISTINA SCUDELARI, CLA´ UDIO FREITAS NEVES, D´EBORA VIEIRA BUSMAN, AND ANDR´E LU´IS SILVA SANTOS (2014) : **Multitemporal Analysis of Coastal Erosion Based on Multisource Satellite Images, Ponta Negra Beach, Natal City, Northeastern Brazil.** *Marine Geodesy*, 0:1–25

time and interpolate them to the location of their study sites. Offshore wave data (wave height, period and direction) may be obtained from offshore wave buoy and a nearshore significant wave height is found using a Simulating WAves Nearshore (SWAN) model[8]. This model transforms wave characteristics from the offshore measurement station to the tip of the site.

2- Morphology data

- Beach profiles: slope information;
- Equilibrium Beach Profile

Beach slope may be retrieved using different methods. In consistency with historical data, some information, parameters may be supposed.

1.2.5 Currently known issues

The availability of satellite data is not uniform for all the locations, and so the time horizon of the analysis is not everywhere the same. In some locations the scarce availability of satellite observations combined with poor observation condition do not allow a satisfactory determination of the land-water transitions. Crucially, an investigation of the full range of temporal scales that can be resolved using satellite-derived shorelines is lacking.

The USGS/DSAS investigation of the differing temporal scales of potential shoreline change with a simple method as least square approximation on time series shorelines causes some issue. In order to monitor coastal evolutions characterized by a time series of SDS positions, the SDS vector is projected along the system of transects. This way the distance between the transect origin and the intersection point of the SDS with a transect is obtained. This distance is proposed to serve as a coastal indicator and changes in this distance over time reveal information on the dynamics at the

[8] Booij, N., Ris, R., Holthuijsen, L.H. (1999). A third-generation wave model for coastal regions. I- Model description and validation. *J. Geophys. Res*. **104**, 7649–7666.

shoreline. This is consistent with the procedure used in the coastal monitoring calculation application. But it is normally assumed that the situation is completely two-dimensional: the profile of a sandy beach may be modified by longshore sediment transport and simultaneously by cross-shore sediment transport. However, different mechanisms contribute to the resulting sediment transport[9]. Moreover, the choice of using transect perpendicular to a based line and comparing its intersection with the time series of shorelines implies a comparison of unrelated points. The intersection between the transect and the first shoreline does not automatically correspond to the intersection with a second shoreline.

The knowledge of beach profiles is needed to realize an estimation of the transported volumes, however, the information on the slope of the beach is not available for the same times the satellite image was taken, and its value changes over time.

In cases we only have a BTM (Bathy Topo Model) incomplete, imprecise (unsure, ill-define) we can use a (equivalent) Equilibrium Beach Profile (EBP) to estimate the volumes of sediment transferred.

1.3 Potential Solutions

A calculation method of beach profile is needed to estimate erosion volumes. Several approaches have been pursued in an attempt to characterize equilibrium beach profiles. An analysis of numerous beach profiles along the US coast fitted using a least squares procedure lead to an estimation of water depth according to sediment characteristics and waves energy[10].

$$h = Ay^n$$

Eq 1

9 Fredsøe Jørgen, Deigaard Rolf (1992): Mechanics of coastal sediment transport. Advanced series on Ocean Engineering. Vol. 3. World Scientific

10 DEAN, R.G., 1977. Equilibrium Beach Profiles: U.S. Atlantic and Gulf Coasts. Department of Civil Engineering, Ocean Engineering Report No. 12, *University of Delaware*, Newark, Delaware.

With *h* is the water depth at a seaward distance *y*, and *A* is a scale factor which depends primarily on sediment characteristics and energy dissipation. A central value of n = 2/3 is generally used.

An unrealistic property of the form of the equilibrium beach profile represented by Eq. 1 is the predicted infinite slope at the shoreline. Moreover, large slopes induce correspondingly large gravity forces which are not represented in Eq. 1. A slight modification to include gravitational effects gives the following equation:

$$y = \frac{h}{m} + \frac{1}{A^{3/2}} h^{3/2}$$

In shallow water, the first term dominates in the **Error! Reference source not found.** equation[11]. Then, we have:

$$h = my$$

Eq 2

i.e. the beach face is of uniform slope *m*, consistent with measurements in nature[12].

In deeper water, the second term dominates which leads to the following simplification:

[11] Robert G. Dean (1991): Equilibrium Beach Profiles: Characteristics and Applications. *Journal of Coastal Research*, 7-1, 53-L.

[12] Umut Türker, M. Sedat Kabdasli (2009): The shape parameter and its modification for defining coastal profiles. *Environ Geol,* **57**:259–266

$$h = Ay^{2/3}$$

Eq 3

But, following this point of view, estimating the profile scale factor *A*, a function of wave energy dissipation, is a complex task (see Aragonés et al 2016)[13].

1.4 Product Specifications

The process will provide 3D coastal erosion information using the changes observed in the position shoreline through a time series analysis. The product would be an information about volumetric changes for a beach transect or all an area for a given time range.

[13] L. Aragonés, J.C. Serra, Y. Villacampa, J.M. Saval, H. Tinoco (2016): New methodology for describing the equilibrium beach profile applied to the Valencia's beaches. *Geomorphology* **259** (2016) 1–11

2 Algorithm Description

(algorithm = scheme for effective calculability as a calculation shall terminate in a limited time and with a limited number of steps)

2.1 Data Processing outline

2.1.1 Sketch of the computer program

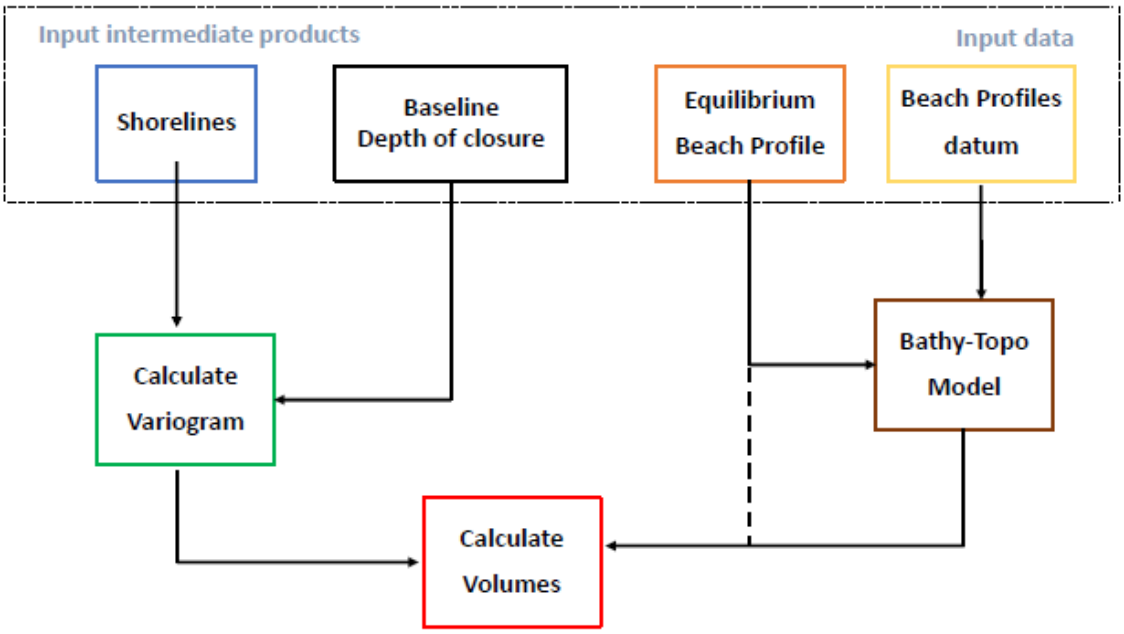

Figure 2.1: Sketch of the computer program for erosion rate calculation

2.1.2 Pre-requisite

A methodology based on a beach profile requires the definition of a limiting depth: The Depth of Closure (DoC) some analysis have been conducted taken into account different timescale ranges[14].

Historically, in Coastal engineering two zones are considered with different levels of morphodynamic activity: a dynamically active region (coastal zone) with significant vertical movement of the beach profile and an inactive region nearer the sea (Shoal Zone) in which vertical movement is lower and whose outer limit is the offshore point.

Therefore, we can consider the depth of closure DoC as the limit of the equilibrium profile and the most suitable depth for the design of beach nourishments[14].

2.2 Algorithm Input

The erosion rate processor needs in input time series of shoreline.

Riazi & Türker (2017)[15] proposed a boundary-based A (beach profile scale factor) determination method. The profile scale factor *A* is proposed in term of "Depth of Closure". In a 2D Cartesian coordinate system, where the horizontal axis is the distance from the shoreline positive seaward *y*, and the vertical axis is the depth of the water (*h*) positive downwards, within the surf zone, the shoreline with the coordinate of (0,0) and the depth of closure with the coordinate (yc , hc) are considered as two common coordinates with slight water depth variation. Then, at the depth of closure we have:

$$A_c = h_c y_c^{-2/3}$$

Eq 4

where *A*c is the boundary-based profile scale factor.

Introducing $y^* = \frac{y_i}{y_c}$ and $h^* = \frac{h_i}{h_c}$

where yi is the horizontal distance of a point within the profile to the origin point of the profile, positive seawards.

[14] Dean, R.G., 2003. Beach nourishment theory and practice. Advanced Series on Ocean Engineering vol. 18. World Scientific Publishing Co., pp. 34–37.

[15] Amin Riazi & Umut Türker (2017): Equilibrium beach profiles: erosion and accretion balanced approach. *Water and Environment Journal* - VC 2017 CIWEM. 1

The main advantage of normalized coordinate system is that the value of *Ac* calculated through Eq. 3

where Ac is the boundary-based profile scale factor.

will always be equal to 1 and therefore Eq. 2 will be independent of A. Thus, the analytical approach for all kinds of EBPs in normalized coordinate system can be simplified to:

$$h^* = (y^*)^{2/3}$$

Eq 5

In this approach, by neglecting the effect of sediment compression, the amount of sediment eroded should be equal to the amount of sediment accreted.

2.3 Theoretical Description of the models in background of the procedure

2.3.1 Physical Description

Shoreline variations for a given time range allow us to access to the shore volumetric changes.

In order to identify the strengths and limitations of the satellite-derived method in capturing typical sub-annual and inter-annual shoreline variations at any site of interest, a more advanced analysis is needed. Hereafter, we propose to tackle the problem by following the geostatistical approach of Vos et al (2019)[16].

[16] Kilian Vos, Mitchell D. Harley, Kristen D. Splinter, Joshua A. Simmons, Ian L. Turner (2019): Sub-annual to multi-decadal shoreline variability from publicly available satellite imagery. *Coastal Engineering* **150**, 160–174

2.3.2 Mathematical Description and calculation procedures

The empirical semi-variogram estimates typical magnitude of change between pairs of points at a temporal lag τ *(*i.e., timescale). The empirical semi-variance (in units of m^2) is computed from the time-series of shoreline cross-shore displacement *d* (*t*):

$$\gamma(\tau) = \frac{1}{2N(\tau)} \sum_{i=1}^{N(\tau)} [d(t+\tau) - d(t)]_i^2$$

Eq 6

were *N* (τ*)* denotes the number of data pairs at lag τ .

A variogram is presented as a graph (figure 2.2), where the calculated variogram values (dots) represent the experimental variogram.

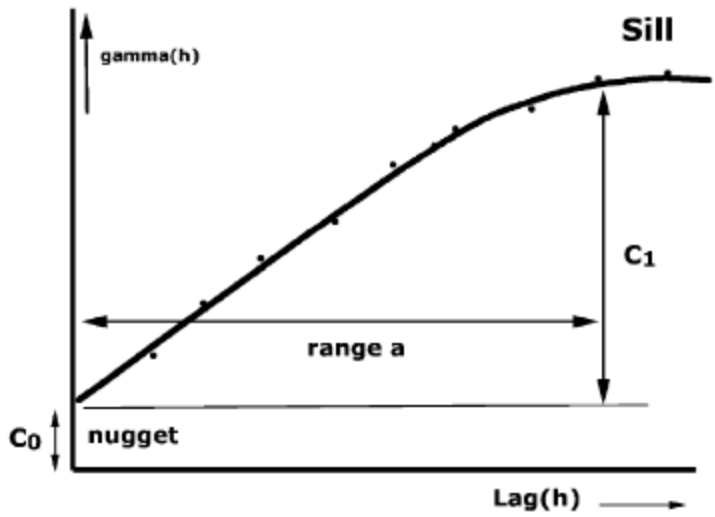

Figure 2.2: Experimental variogram (black dots) and theoretical variogram (curve).

Hereby, the 'sill' is the total variance of the variable, the 'range' is the maximal spatial extent of spatial correlation between observations of the variable and the 'nugget' is the random error.

2.3.3 Acceptance of the Models

The time-spatial variation of coastal erosion measurements is complex but is not (generally) unstructured. It is almost always spatially dependent on some scale. Long term variation (the trend) may then be overlain by more or less random short-term variation. The whole can be described by a

variogram that summarizes the expected tendency. This feature can be found in many scientific disciplines: Air Quality (Wong et al. 2004)[17], Coastal Morphology (Verfaillie et al, 2006)[18] and in a general way to apprehend the natural phenomena (Goovaerts 1997)[19].

2.3.4 Error estimation and uncertainty

The fitting of a theoretical variogram (curve) is an important step in the variogram analysis. The theoretical variogram can be composed of nested models or structures. Common models are the nugget model, spherical model, exponential model, Gaussian model and power model. Direction dependant variograms can be set up in the case of anisotropic variability. The formulas of these models can be found in Wackernagel (1998)[20].

2.4 Algorithm output

The empirical semi-variogram at Narrabeen (a beachside suburb in northern Sydney) field survey transect NA1, converted to units of metres ($\Upsilon(h)$), is plotted in figure 2.3 and depicts the typical variability spanning 42 years of observations for monthly to decadal timescales at this location. The magnitude of typical shoreline change is shown to increase as lags (timescales) become longer, until becoming asymptotic to a 'sill'.

[17] David W. Wong, Lester Yuan & Susan A. Perlin (2004): Comparison of spatial interpolation methods for the estimation of air quality data. *Journal of Exposure Analysis and Environmental Epidemiology*, **14**, 404–415

[18] Els Verfaillie, Vera Van Lancker, Marc Van Meirvenne (2006): Multivariate geostatistics for the predictive modelling of the surficial sand distribution in shelf seas. Continental Shelf Research, **26**, 2454–2468

[19] Goovaerts, P. (1997): Geostatistics for Natural Resources Evalation. *Oxford University Press*, New York, 483pp.

[20] Wackernagel, H., 1998. Multivariate Geostatistics. Springer, Berlin, 291pp.

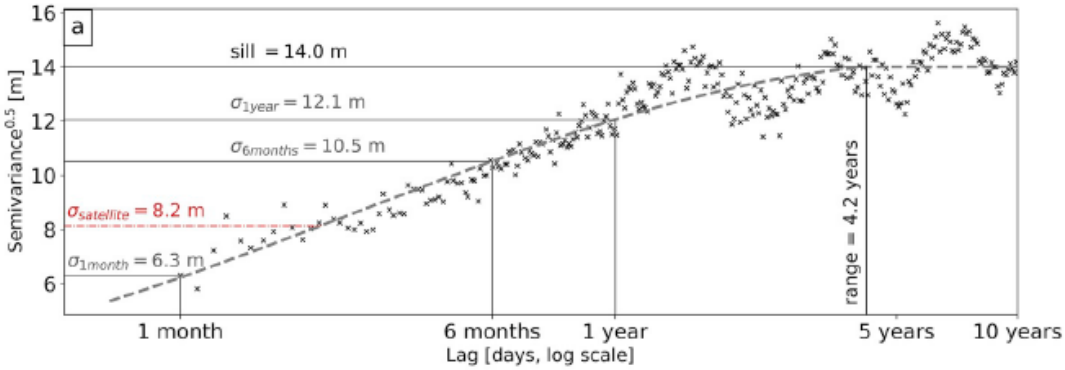

Figure 2.3: Empirical semi-variogram (converted to units of meters) for a transec at Narrabeen-Collaroy (NA1). It shows typical cross-shore shoreline variability at different timescales, from monthly lags to 10 years lags. The dashed grey line is a smooth fit across the data points. The range and sill are also indicated on the figure (in Vos et al, 2019).

The calculation process should be based on exhaustive measurement of the distance between two shorelines.

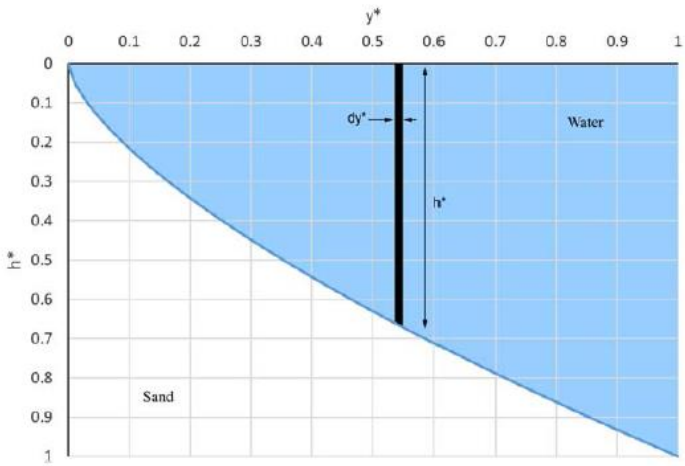

Figure 2.4 : Representation of EBP through Eq. (5). The profile is the lower boundary for the volume of water per unit width above the sand. Given h* as a function of y*, the volume per unit width of water can be calculated by definite integral of y* over the interval of [0, 1] (in Riazi & Türker, 2017).

The volume of water per unit width (α) above the Equilibrium profile given by Eq.4 is calculated as:

$$\alpha = \int_0^1 h^*.dy^*$$

In a normalized coordinate system:

$$\alpha = 0.6\frac{m^3/m}{m^3/m}$$

Suppose we get a satellite Image during an EPB situation. The shoreline and the depth of closure are well recognized. Then, sometime later, we observe a cross shore motion (landward or seaward) of the shoreline equal to ε.

ε must be normalized: $$\epsilon^* = \epsilon/y_c$$

Then, in a foreseeable future, a next situation of an EPB would appear. Thus, the variation of volume per unit width should be:

$$\delta V_\epsilon = \alpha.(\epsilon^*)^{5/3} = \alpha\epsilon^* h_\epsilon^*$$

Practically, this last equation can be used only beyond the nugget distance ε_n detected on the variogram. Note that the nugget distance depends on the choice of the variogram model.

In case of displacement of the shoreline smaller than the nugget distance, the variation of volume per unit could be evaluated by summing on a “nugget triangle”, i.e., assuming that we are then in shallow water and that therefore it is the effect of gravity that dominates and that the depth is given by the linear equation 5 (from Dean, 1991).

At the nugget distance ε_n we have the normalized depth:

$$h_n^* = (\epsilon_n^*)^{2/3}$$

Then regarding the "nugget slope", we have:

$$m_n = \frac{h_n^*}{2\epsilon_n^*}$$

The nugget volume (per unit width) may be estimated as:

$$\delta V_n = \epsilon_n^* . h_n^*$$

Eq 7

2.4.1 Product content

The product will be based on two geometric entities: shoreline and transects.

All information related to erosion rates and shorelines will be linked to these geometric components.

For example, over a reference period Prieto-Campos et al (2018)[21] represent Erosion/accretion rates using proportional symbols, assigning easy-to-interpret colour tones. The colour blue, for example, was thus assigned to sediment accumulation processes, red to erosion processes, and white to zones of sediment stability (figure 2.5).

[21] Antonio Prieto-Campos, Pilar Díaz-Cuevas, Miriam Fernandez-Nunez and José Ojeda-Zújar (2018) Methodology for Improving the Analysis, Interpretation, and Geo-Visualisation of Erosion Rates in Coastal Beaches—Andalusia, Southern Spain. Geosciences 2018, 8, 335

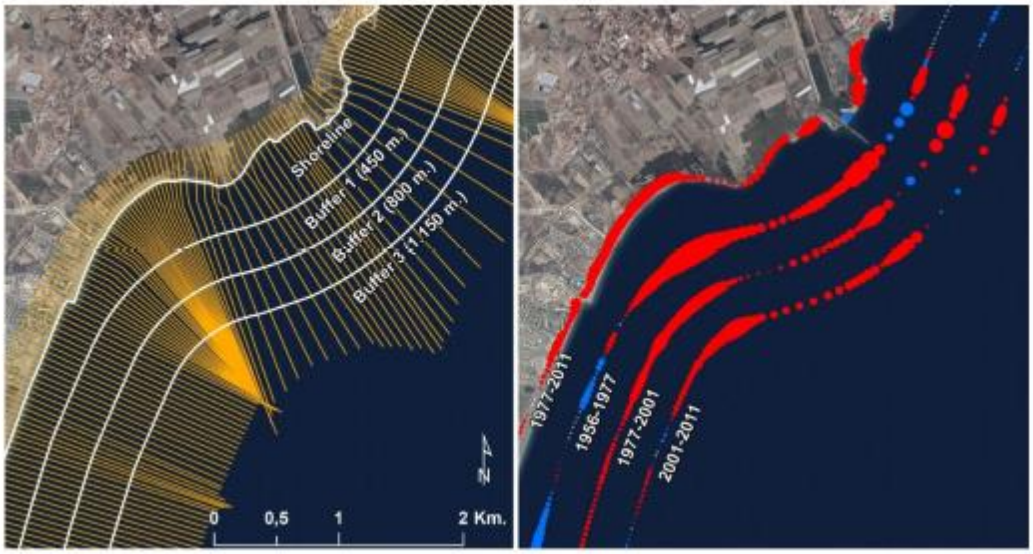

Figure 2.5: Representation of erosion rates on point entities.

On a ROI, the erosion rates can be aggregated for different studied periods. These rates may be resampled to be able to map them in a single static map (cf. figure 2.6).

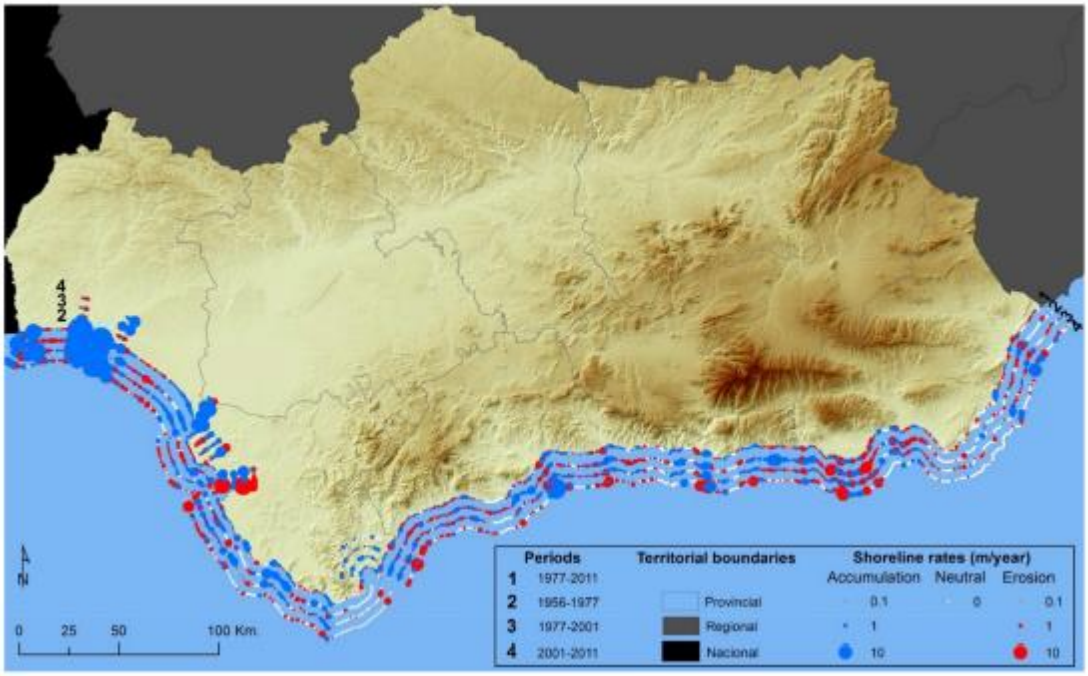

Figure 2.6 : Overall erosion rates estimated for each kilometre of the Andalusian coast (in Prieto-Campos, 2018).

2.4.2 Product organisation

Erosion rate products will be organized in different folder according to the study area. For each area partners will access the erosion rate with all metadata, refer to section 2.4.1.

Calcul du variogram

Calcul du DEM ou calcul de l'Equivalent Equilibrium Beach Profile (EEBP)

Calcul des volumes érodés.

2.5 Algorithm Performance Estimates

2.5.1 Test specification

To quantify the degree to which the satellite-derived shorelines could resolve the observed temporal scales of variability, an analysis of the measurement accuracy relative to the shoreline variability will be performed using the signal-to-noise ratio (SNR) as a measure of how much useful information there is in a system:

$$SNR = \frac{\sqrt{\gamma(lag)}}{\sigma_{sat}} = \frac{\sigma_{lag}}{\sigma_{sat}}$$

Eq 8

Values of SNR > 1 indicate that the shoreline signal is increasingly dominant over the measurement error and hence the satellite-derived measurements are able to distinguish a change in shoreline position. SNR values < 1 meanwhile denote signals that are indistinguishable from measurement noise and thus no physical change can be detected using satellite-derived shorelines at that particular timescale.

2.5.2 Test Datasets

To illustrate the methodology, Vos et al. (2019) used at Narrabeen-Collaroy a total of 502 satellite-derived shorelines between 1987 and 2018.

To identify the timescales at which the shoreline signal can be resolved by the satellite-derived observations, the SNR was computed at each site across a range of temporal scales and the results presented in figure 2.7.

This analysis reveals that no significant difference is observed between the error distribution of data points obtained from Landsat 5, Landsat 7, Landsat 8 and Sentinel-2. This is in spite of pixel resolutions varying in the different satellite missions from 30 m for the older Landsat 5 images to 10 m for the most recent Sentinel-2 data.

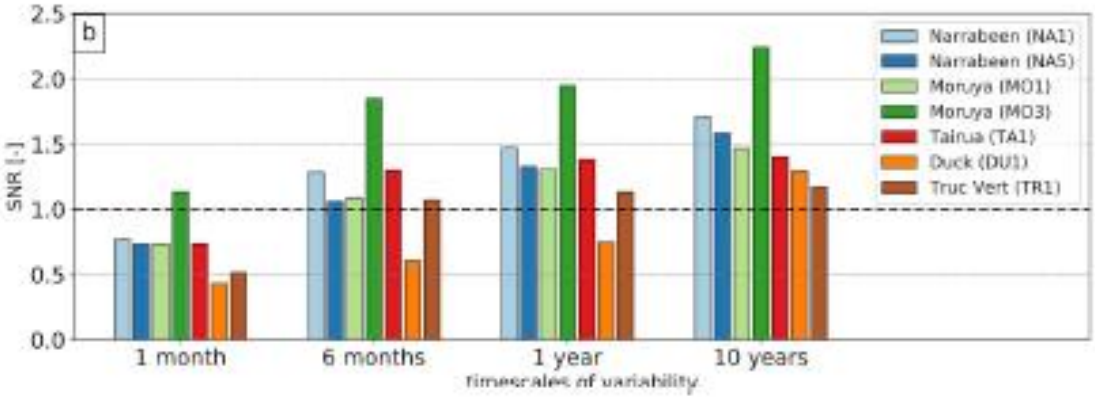

Figure 2.7: Signal-to-noise ratio analysis across different timescales. Values of SNR above the threshold of 1 denote shoreline signals that are increasingly dominant over the measurement error (in Vos et al, 2019)

Satellite derived shorelines have a SNR>1 for timescales longer than 6 months (except for Duck site). This reveals that satellite-derived shorelines can be used to examine intra- and inter-annual shoreline behaviour at a wide range of beaches around the world where a measurable shoreline variance is present.

2.5.3 Verification

Choosing an indicative threshold of 1 for the SNR, whereby the physical change in shoreline position exceeds the measurement error, the semi-variogram will indicates how satellite observations can be

reasonably used to resolve typical variability of more than a time period (ex: 6 months) at diverse sites included in a global study.

2.5.4 Practical Considerations

It is reasonable to speculate that a number of factors could potentially influence the position of shoreline indicator features obtained by digital image analysis. The stage of the tide, beach slope, the prevailing wave energy, and the position of the groundwater exit point are likely to be of significance.

To be complete in next version.

2.6 Products Validation

The products developed in this work have some limitations derived from their two-dimensional (2D) nature (distances measurements), and they should be treated carefully as erosion is a 3D phenomenon (volumetric measurements).

2.6.1 Test specifications

Test Protocols are used to demonstrate that a system meets requirements previously established in specification, design, and configuration documents.

The Test Plan outlines the testing requirements and strategy. The Test Plan may also include the types of testing, descriptions of environments where testing will be performed, who is responsible for testing, equipment or testing that will be used in testing, or other organizational requirements for testing.

Test Protocols are collections of Test Cases which check a specific element of the system. Each test case should include the purpose of the test, any pre-requisites that need to be done before testing, and the acceptance criteria for the test.

2.6.2 Test Datasets

Extensive engineering tests will be conducted to determine compliance with specification requirements (sets by purchaser) to ensure thorough quality controls.

2.6.3 Validation

The accuracy of this product depends strongly on the accuracy of the shorelines provided by the Shorelines Processor which has been extensively validated. A large-scale validation of the present dataset on shoreline dynamics is hampered by the scarcity and heterogeneity of field measurements.

3 Conclusion

i.e. Roadmap for improvements

3.1 Assessment of limitations

In some locations the scarce availability of satellite observations combined with poor observation conditions (e.g. frequent cloud or snow occurrence, or long polar night) do not allow a satisfactory determination of the land-water transitions

Therefore, a set of criteria based on the number of valid observation available, will be set up to identify and filter out these locations (excluding, for example, areas with an insufficient number of valid observations).

As a consequence, the coverage of the global coast is incomplete: only about 86% of the coastline at latitudes below 63 degrees (Mentashi et al,2018)[22].

Another limitation of the study relates to the spatial (30 m) and temporal (8-day cycle or 16 days when two satellites operate concurrently) resolutions of the satellite imagery, which prevent capturing small-scale or short terms changes.

[22] Lorenzo Mentaschi, Michalis I. Vousdoukas, Jean-Francois Pekel, Evangelos Voukouvalas & Luc Feyen (2018): Global long-term observations of coastal erosion and accretion. www.nature.com/scientificreports ***8**:12876*

3.2 Mitigation

4 References

5 Appendix

End of Document